

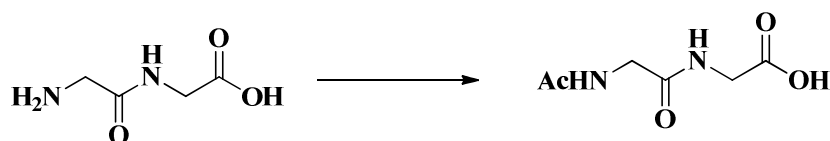
Supporting Information:

Reversal of the Hofmeister Series: Specific Ion Effects on Peptides

Jana Paterová,¹ Kelvin B. Rembert,² Jan Heyda,³ Yadagiri Kurra,² Halil I. Okur², Wenshe R. Liu², Christian Hilty,² Paul S. Cremer,^{2*} and Pavel Jungwirth^{1*}

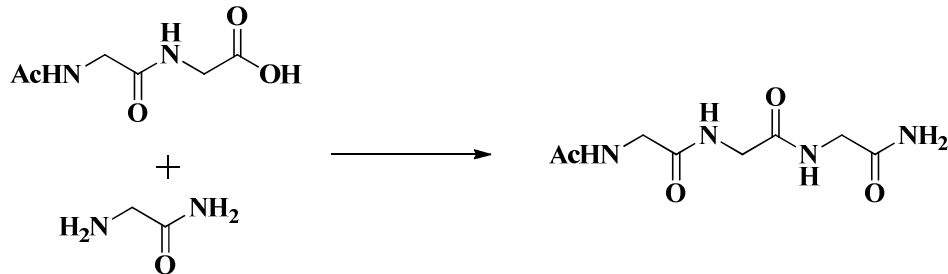
¹*Institute of Organic Chemistry and Biochemistry, Academy of Sciences of the Czech Republic, Flemingovonám. 2, 16610, Prague 6, Czech Republic,* ²*Department of Chemistry Texas A&M University, 3255 College Station, TX 77843, USA,* ³*Soft Matter and Functional Materials, Helmholtz-Zentrum Berlin, Hahn-Meitner Platz 1, 14109 Berlin, Germany*

Synthesis of N-Acetyldiglycine¹



Diglycine was dissolved in a minimum amount of saturated NaHCO₃ solution. Two molar equivalents of acetic anhydride were added. After 10 min at room temperature, the reactant was heated to the boiling point for 3 min in order to hydrolyze the unreacted acetic anhydride. The acetylated peptide was chromatographically purified using a Dowex-50 column. After the reactant was absorbed onto the column, it was washed with water. The first column volume of elutant was discarded, and the next 1.5 column volumes of eluent were collected and lyophilized.

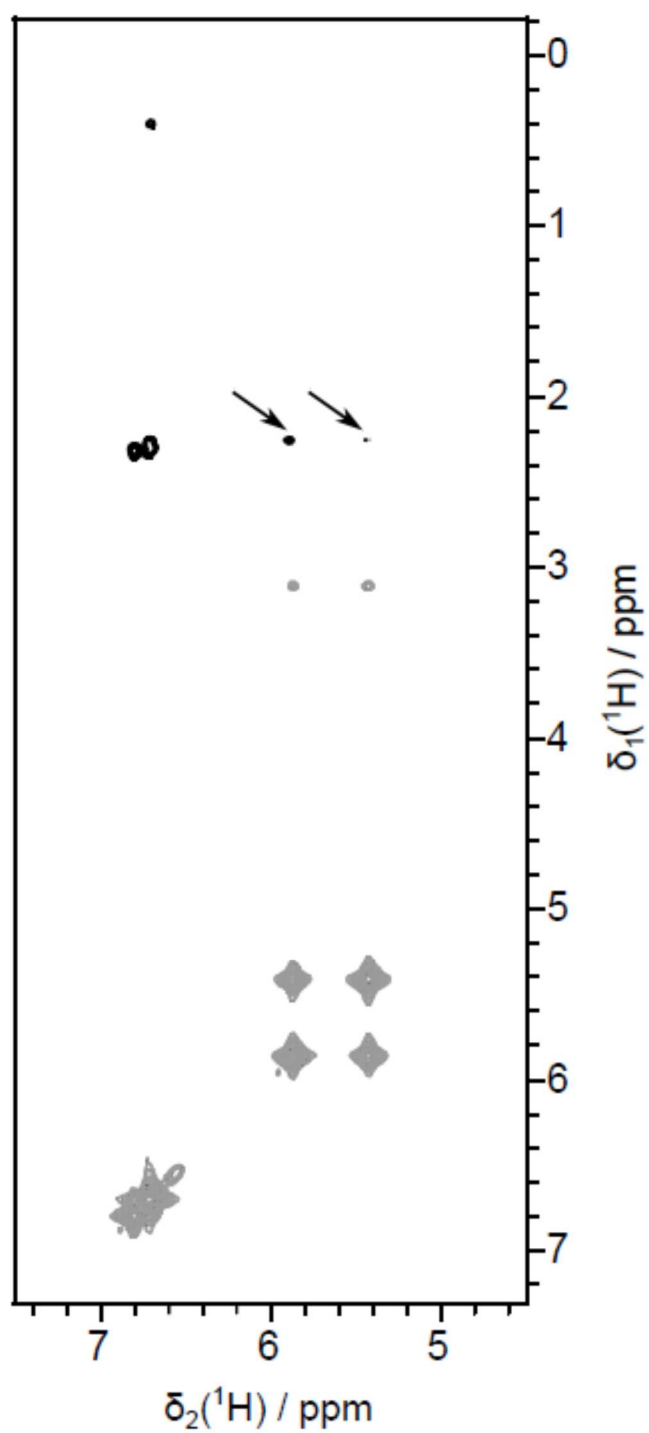
Synthesis of *N*-Acetyltriglycinamide²



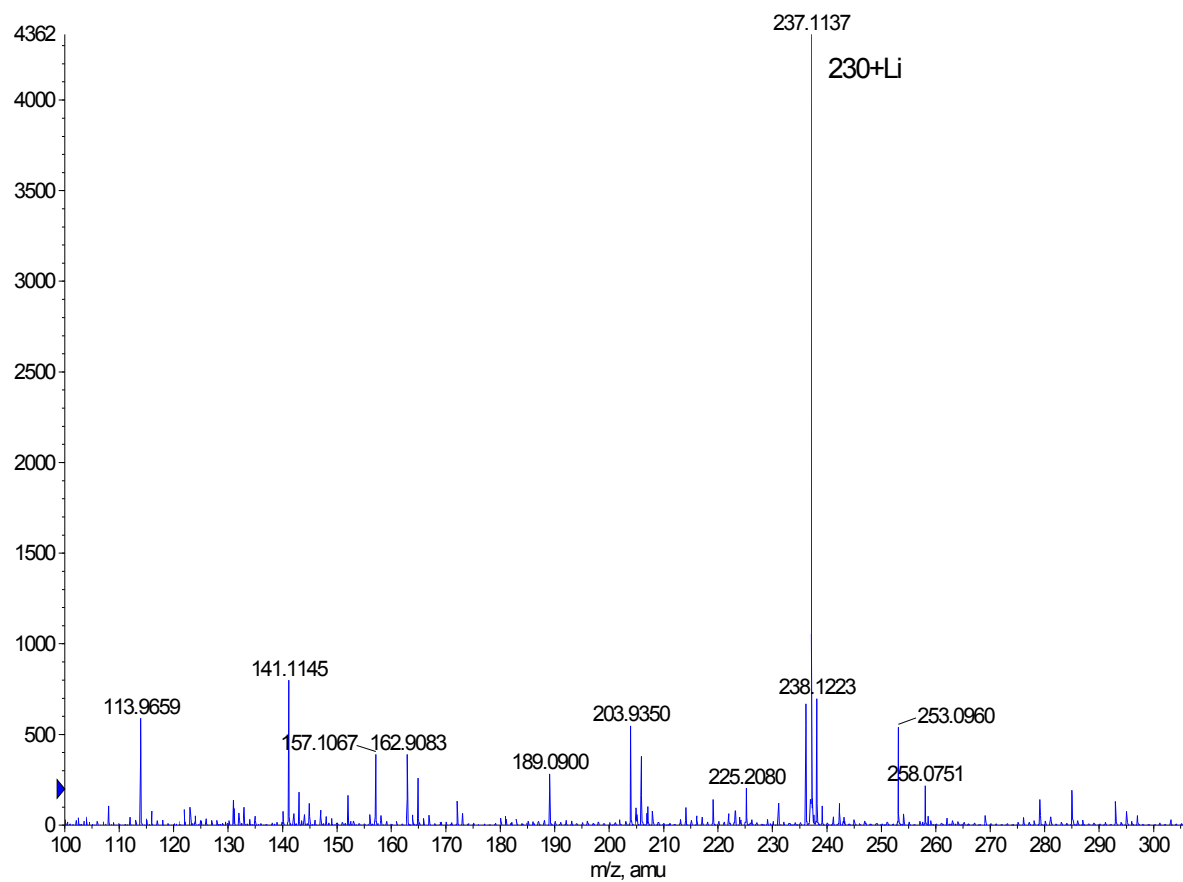
A mixture of glycylglycine (1.5g, 13.69 mmol) and dry DMF was neutralized with Et₃N (1.49g, 13.66mmol). After stirring for 10 min, *N*-acetyl diglycine (2g, 13.69mmol) was added and stirring was continued for another 10 min followed by the addition of 1-hydroxybenzotrazole hydrate (2.03g, 15.03mmol). After cooling to -10 °C, a solution of DCC (3.1g, 15.04mmol) in dry CH₂Cl₂ was added in small portions and the mixture was stirred for 2h at -10 °C. After warming to room temperature, the suspension was stirred for 6h and left overnight without stirring. The solid was separated, stirred in 500 ml of boiling EtOAc, re-separated and dried in air. This peptide was purified by Dowex-50 column chromatography.

N and *C* terminus modification verification

As noted in the main text, Nandi and Robinson previously attempted to modify the *C*-terminus of triglycine through esterification.^{3,4} This attempt was unlikely to have been successful, although proper spectroscopic verification by the authors was not reported. Their experimental results for the solubility of capped triglycine as a function of different sodium salts are most consistent with an anionic species whereby only the *N*-terminus was properly capped. The difficulty in capping the *C*-terminus of the small triglycine peptide may arise from the reactivity of the *C*-terminal acyl group resulting in hydrolysis. After several failed attempts at capping the *C*-terminus through esterification procedures similar to those reported by Nandi and Robinson, we found amidation to be a more stable modification. Proper amidation of the *C*-terminus was confirmed by NMR and mass spectrometry as follows. First, nuclear Overhauser effect spectroscopy (NOESY) experiments were performed (Figure S1). The black arrows in the figure denote the positions of the NOE cross peak for the correlation between the amide protons on the *C*-terminus and α -proton number 3. These data were processed with Computer Aided Resonance Assignment⁵ (CARA) software according to the literature.⁶ Next, electrospray ionization (ESI) time-of-flight (TOF) mass spectrometry was employed to further confirm amidation. The corresponding acetylated and amidated modified molecule complexed with Li⁺ displays a mass peak at 237.1137 Da (Figure S2).



FigureS1. NOESY spectrum of 50mM N-acetyltryglycinamide in purified water. Positive contours are shown in gray, and negative contours in black



FigureS2.ESI TOF mass spectrum of a 100uM sample of *N*-acetyltriglycinamide in methanol.

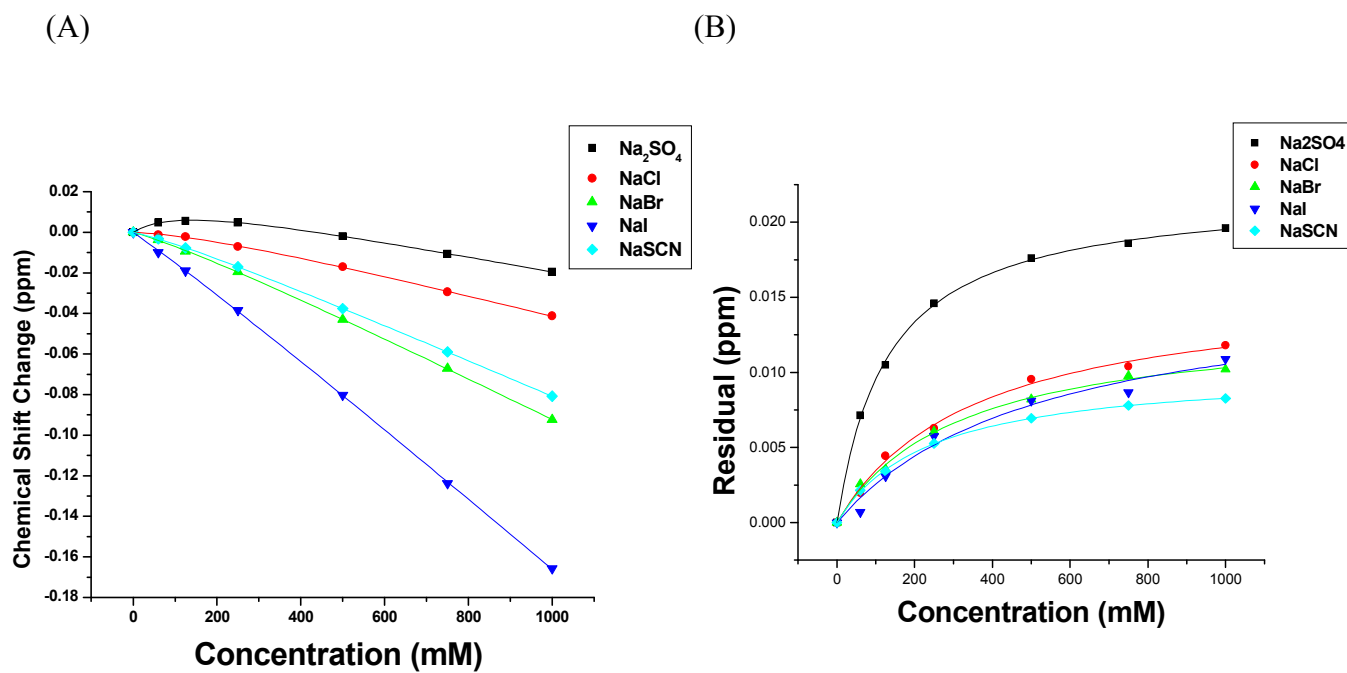
Chemical shift data for Additional Protons

The chemical shift changes of the amide protons were measured as a function of salt concentration analogously to the CH protons presented in the body of the paper. Figure S3A shows the chemical shift changes of the NH proton from the middle glycine residue of triglycine as a function of salt concentration versus five different sodium salts. Figure S3B shows the same data after the linear portion has been subtracted. The results reveal apparent Langmuir isotherm behavior for the chemical shift changes for all salts. In contrast to the data for the α -protons (Figures 4 & 5, main text), sulfate shows a shift in the same direction as the other four anions. It should be noted that data for the positively charged *N*-terminal amino group as well as the amide backbone from the *C*-terminal glycine could not be reliably obtained as these protons exchanged sufficiently rapidly with water.

Figure S4A shows the chemical shift changes of the 3 backbone amide protons as well as the one from the *C*-cap of *N*-acetyl triglycinamide as a function of salt concentration for Na₂SO₄. Amide 1, 2, and 3 correspond to the positions of the amide protons from the *N*-terminus to *C*-terminus on the tripeptide structure analogous to the numbered α -protons as seen in the main text (Figures 4). Figure S4B plots the same data after subtraction of the linear portion. These results reveal apparent binding isotherm behavior. Amide protons 1, 2, and 3 shift in the same positive direction while the *C*-terminus amide protons shift in the opposite direction. It should be noted that amide protons 1 and 3 were unresolved in the NMR spectrum.

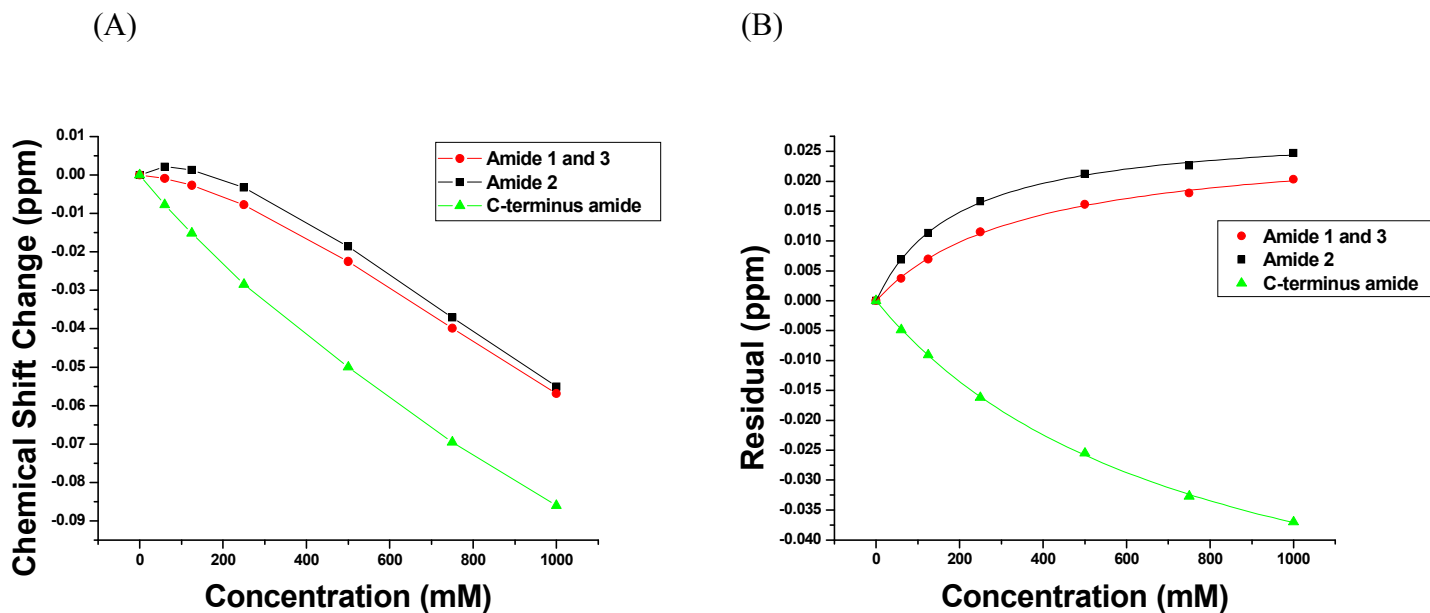
The chemical shift changes of amide protons 1, 2, and 3 and of the *C*-terminus cap were also plotted for NaCl, NaBr, NaI, and NaSCN (Figures S5-8). In every case the chemical shift decreased monotonically, shifting to lower ppm values. These data are analogous to chemical shift changes of the *N*-terminal methyl protons of *N*-acetyl triglycinamide versus salt concentration for the 5 sodium salts in Figure S9.

Data for sodium salts with an NH Proton of triglycine



FigureS3. (A) Chemical shift change of one of the amide protons in triglycine as a function of salt concentration. (B) Plots the residual chemical shift change after linear subtraction. Curves were best fit to Langmuir Isotherms.

Data for Na₂SO₄ with NH Protons of N-acetyltriglycinamide



FigureS4. (A)Chemical shift change of the three backbone amide protons and the C-terminal amide protons of *N*-acetyltriglycinamide as a function of sodium sulfate concentration. (B) Residual chemical shift changes after subtraction of the linear contribution. Curves were best fits to Langmuir isotherms.

Data for NaCl with NH Protons N-acetyltriglycinamide

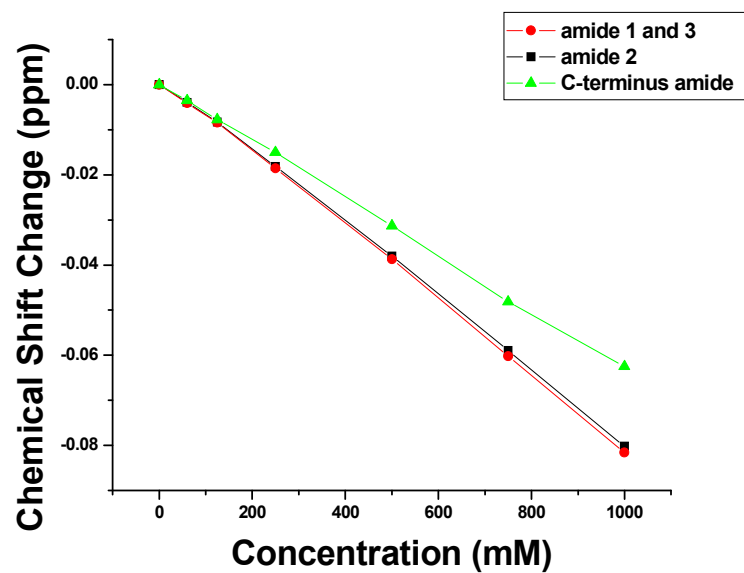


Figure S5. Chemical shift change of the three backbone amide protons and the C-terminal amide proton of *N*-acetyltriglycinamide as a function of sodium chloride concentration. Data points are connected to guide the eye.

Data for NaBr with NH Protons of N-acetyltriglycinamide

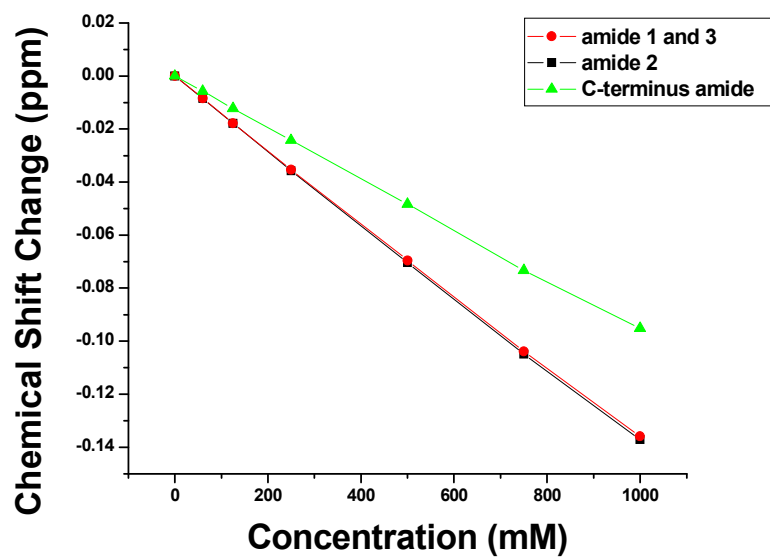


Figure S6. Chemical shift change of the three backbone amide protons and the C-terminal amide protons of *N*-acetyltriglycinamide as a function of sodium bromide concentration. Data points are connected to guide the eye.

Data for NaI with NH Protons of N-acetyltriglycinamide

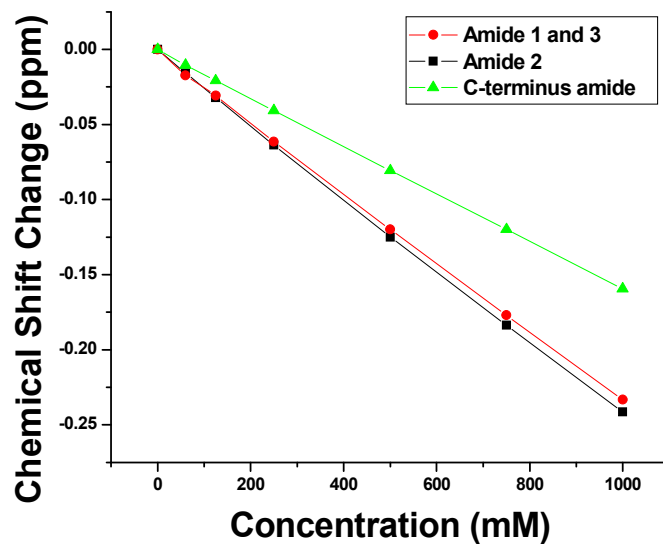


Figure S7. Chemical shift change of the three backbone amide protons and the C-terminal amide protons of *N*-acetyltriglycinamide as a function of sodium iodide concentration. Data points are connected to guide the eye.

Data for NaSCN with NH Protons of N-acetyltriglycinamide

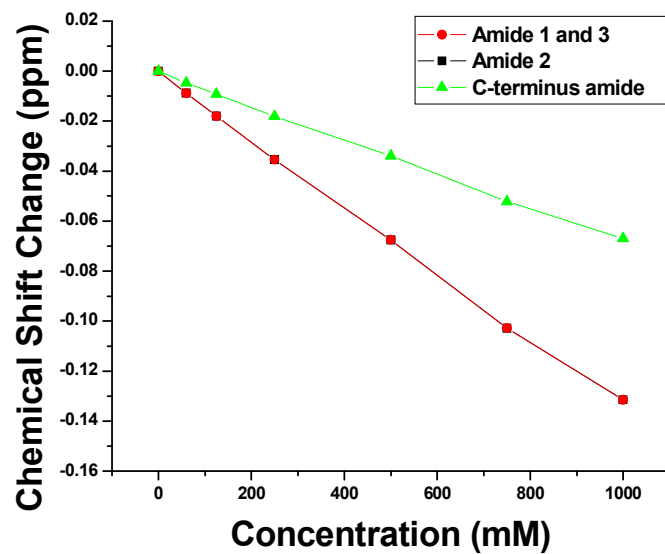


Figure S8. Chemical shift change of the three backbone amide protons and the C-terminal amide protons of *N*-acetyltriglycinamide as a function of sodium thiocyanate concentration. Data points are connected to guide the eye.

Data for salts with CH₃ Protons of N-acetyltriglycinamide

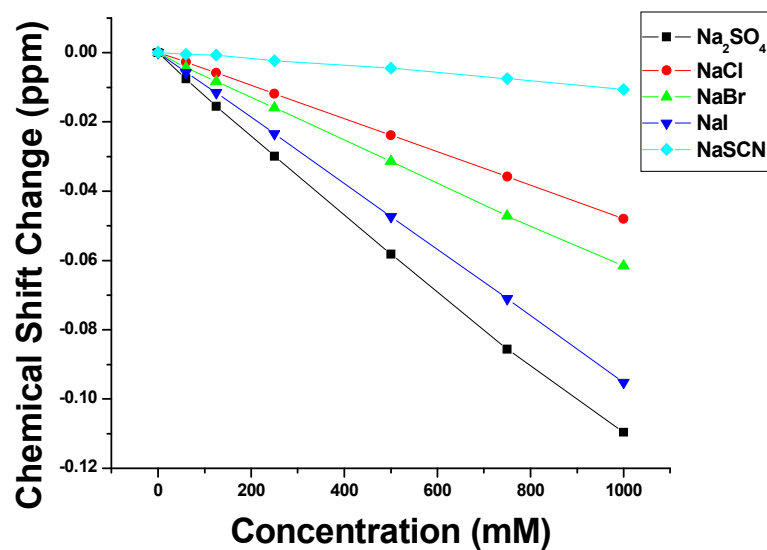


Figure S9. Chemical shift change of the methyl protons of the *N*-terminal cap of *N*-acetyltriglycinamide as a function of salt concentration. Data points are connected to guide the eye.

Data for H₂O Protons as a function of Na₂SO₄ Concentration

Chemical shift data for the bulk water from the capped and uncapped GGG experiments could also be abstracted. The data reveal that the chemical shift is nearly linear for these protons as a function of Na₂SO₄ concentration for both cases.

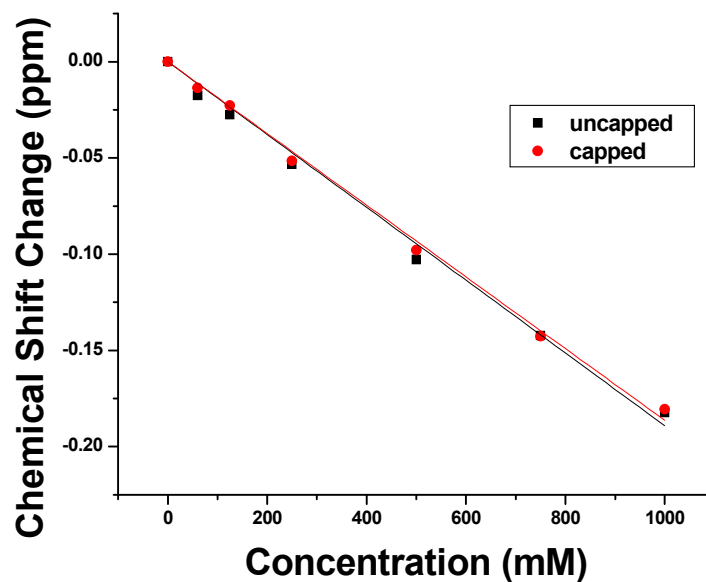


Figure S10. Chemical shift change of aqueous sodium sulfate water protons in the presence of uncapped and end-capped triglycine, black and red respectively.

Sodium Sulfate effect on triglycine and end-capped triglycine structure

Chemical shift changes of the α -protons (Figures 4&5 main text) and the amide protons (Figures S3&S4) show Langmuir isotherm behavior for triglycine and *N*-acetyltriglycinamide in the presence of Na_2SO_4 , which might suggest direct interactions with the peptide backbone. However, sodium sulfate is known to promote protein folding and might change the structure of the capped and uncapped forms of triglycine or its solvation shells via anion exclusion. To further test these ideas, FTIR spectra of *N*-acetyltriglycinamide were measured in D_2O and in 1M Na_2SO_4 in D_2O (Figure S11). The FTIR spectra show the characteristic amide I band at 1642 cm^{-1} and a broad shoulder at 1710 cm^{-1} which is due to the amidation at the C-terminus of the molecule. The amide II band appears as a doublet at 1408 cm^{-1} and 1477 cm^{-1} due to mixing between the C-N stretching and CH_3 bending modes. Moreover, the amide III band can be seen at 1338 cm^{-1} .⁷⁻⁹ Overall, these two spectra show identical peak positions and intensities within experimental error.

By contrast with the capped triglycine data, the vibrational spectra of uncapped triglycine in D_2O and in 1M Na_2SO_4 in D_2O show some subtle spectral differences (Figure S12). The amide I band of triglycine appears as a doublet at 1681 cm^{-1} and 1650 cm^{-1} . The higher frequency peak is from the *N*-terminus and the lower one is characteristic of the amide I band.¹⁰ The absorption peaks at 1593 cm^{-1} and 1395 cm^{-1} are the asymmetric and symmetric carboxylate stretches and the peaks at 1482 cm^{-1} and 1314 cm^{-1} are the amide II and amide III bands, respectively.⁹ All these spectral features, excluding the 1681 cm^{-1} band, shift less than 2 wavenumbers in the presence of SO_4^{2-} ions. The 1681 cm^{-1} shifts approximately 4 cm^{-1} . The larger shift of this band should be due to ion pairing between NH_3^+ and SO_4^{2-} . On the other hand, the smaller shifts of the other peaks may be the result of small structural changes in the peptide caused by the ion pairing. Nonetheless, FTIR does not have the spectral resolution to definitively resolve such small changes. These results, especially from the capped triglycine, seem to rule out the idea that SO_4^{2-} binds directly with uncharged amide moieties. Moreover, thermodynamic data from Von Hippel and coworkers using column chromatography demonstrate that SO_4^{2-} ions are excluded from amide protons of polyacrylamide gels.¹¹ Therefore, the NMR shifts are likely caused by changes in peptide conformation or perhaps its adjacent water structure due to the exclusion of Na_2SO_4 .

To rule out the possibility of a peptide self-association effect, titrations of 1mM triglycine with Na_2SO_4 were carried out (Figure S13). The results are mostly identical to the titrations of 50mM triglycine with Na_2SO_4 (Figure 4 & 5, pp. 27-28).

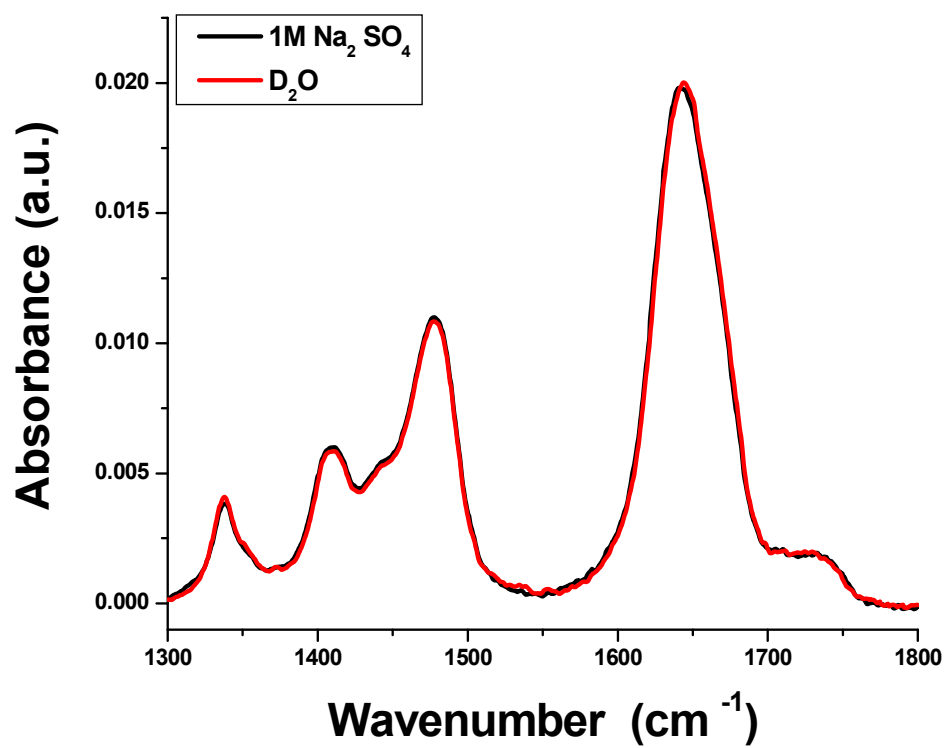


Figure S11. FTIR spectra of 100mM *N*-acetyltryglycinamide in D₂O and 1M Na₂SO₄ in D₂O, red and black respectively.

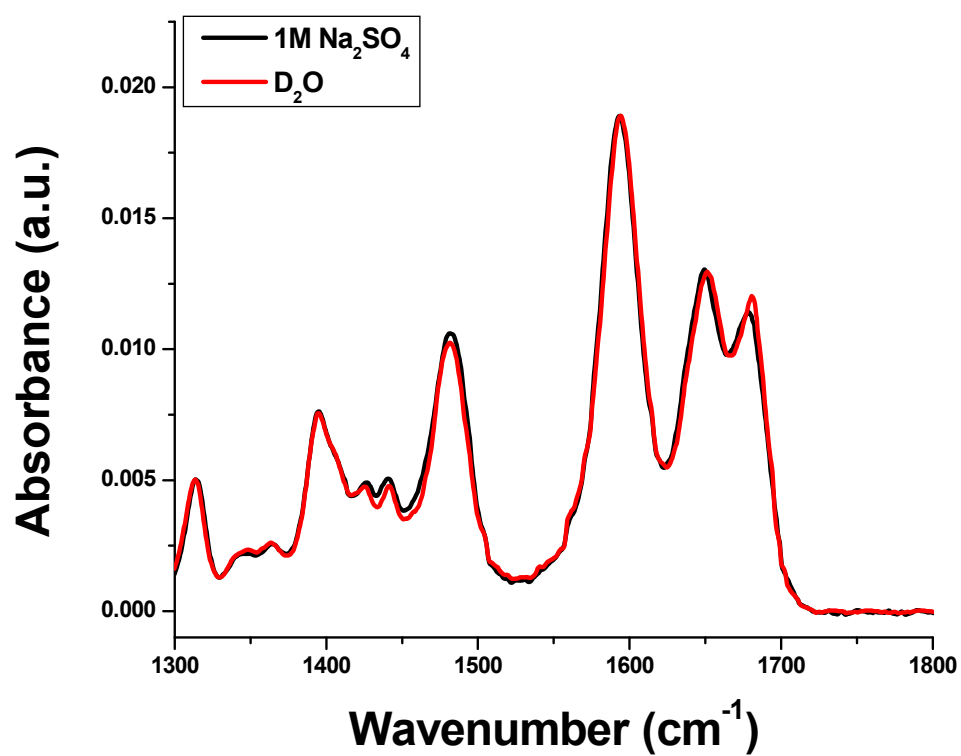


Figure S12. FTIR spectra of 100mM triglycine in D₂O and 1M Na₂SO₄ in D₂O, red and black respectively.

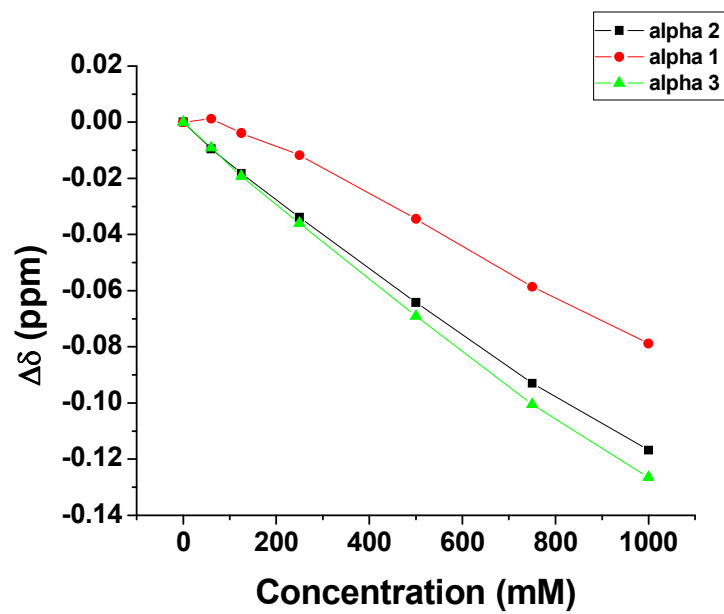


Figure S13. Chemical shift changes of the α -protons of 1mM triglycine as a function of Na_2SO_4 concentration. Data points are connected to guide the eye.

Additional results from NMR data fits

N-Ac-GGG-NH ₂				GGG			
Na ⁺ counter-anion	δ_{\max} (ppm)				δ_{\max} (ppm)		
	α -proton 1	α -proton 2	α -proton 3		α -proton 1	α -proton 2	α -proton 3
SO ₄ ²⁻	-	-	-		0.0084 ± 0.000035	-	-
Cl ⁻	-	-	-		0.0066 ± 0.00067	-	-
Br ⁻	-	-	-		0.026 ± 0.0026	-	-
I ⁻	0.027 ± 0.0045	-	-		0.064 ± 0.022	-	-
SCN ⁻	0.023 ± 0.0085	0.010 ± 0.031	-		0.033 ± 0.0044	0.01497 ± 0.44887	-

Table S1: Fitted values and associated error for the chemical shift, δ_{\max} , from equation 1 for alpha protons in different aqueous salt solutions with glycylglycylglycine and *N*-acetyl-glycylglycylglycinamide.

N-Ac-GGG-NH ₂				GGG			
Na ⁺ counter-anion	c (ppm/mol*L ⁻¹)				c (ppm/mol*L ⁻¹)		
	α -proton 1	α -proton 2	α -proton 3		α -proton 1	α -proton 2	α -proton 3
SO ₄ ²⁻	-1.1x10 ⁻⁴ ± 1.4x10 ⁻⁶	-1.14x10 ⁻⁴ ± 2.1x10 ⁻⁶	-1.2x10 ⁻⁴ ± 2.7x10 ⁻⁶		-8.9x10 ⁻⁵ ± 1.5x10 ⁻⁶	-1.2x10 ⁻⁴ ± 2.9x10 ⁻⁶	-1.3x10 ⁻⁴ ± 2.8x10 ⁻⁶
Cl ⁻	4.8x10 ⁻⁵ ± 1.5x10 ⁻⁷	-5.1x10 ⁻⁵ ± 2.2x10 ⁻⁷	-5.7x10 ⁻⁵ ± 3.5x10 ⁻⁷		-3.4x10 ⁻⁵ ± 2.8x10 ⁻⁶	-5.3x10 ⁻⁵ ± 6.0x10 ⁻⁷	-6.3x10 ⁻⁵ ± 4.5x10 ⁻⁷
Br ⁻	-6.1x10 ⁻⁵ ± 3.1x10 ⁻⁷	-6.5x10 ⁻⁵ ± 8.3x10 ⁻⁷	-7.3x10 ⁻⁵ ± 9.4x10 ⁻⁷		-4.7x10 ⁻⁵ ± 1.1x10 ⁻⁵	-6.7x10 ⁻⁵ ± 2.1x10 ⁻⁷	-7.9x10 ⁻⁵ ± 3.8x10 ⁻⁷
I ⁻	-1.0x10 ⁻⁴ ± 2.0x10 ⁻⁵	-9.8x10 ⁻⁵ ± 3.9x10 ⁻⁷	-1.1x10 ⁻⁴ ± 3.7x10 ⁻⁷		-9.0x10 ⁻⁵ ± 4.7x10 ⁻⁷	-7.1x10 ⁻⁵ ± 9.5x10 ⁻⁵	-1.0x10 ⁻⁴ ± 4.1x10 ⁻⁷
SCN ⁻	-1.8x10 ⁻⁵ ± 3.7x10 ⁻⁵	-1.5x10 ⁻⁵ ± 1.3x10 ⁻⁴	-1.8x10 ⁻⁵ ± 2.9x10 ⁻⁷		-1.2x10 ⁻²³ ± --	-1.8x10 ⁻⁵ ± 3.8x10 ⁻⁵	-2.6x10 ⁻⁵ ± 2.0x10 ⁻⁷

Table S2: Fitted values and associated error for c from equation 1 for alpha protons in different aqueous salt solutions with glycylglycylglycine -and *N*-acetyl-glycylglycylglycinamide.

Additional results from MD simulations

GGG		Extended	Partially folded	Folded
Terminated	Na ₂ SO ₄	64%	23%	13%
	NaCl	58%	27%	15%
	NaBr	61%	24%	15%
	NaI	58%	25%	17%
	NaSCN	65%	19%	17%
Non-terminated	Na ₂ SO ₄	66%	20%	14%
	NaCl	69%	21%	10%
	NaBr	68%	21%	11%
	NaI	67%	22%	11%
	NaSCN	60%	28%	12%

Table S3: Relative abundancies of extended, partially folded, and folded structures of terminated and non-terminated GGG from MD simulations.

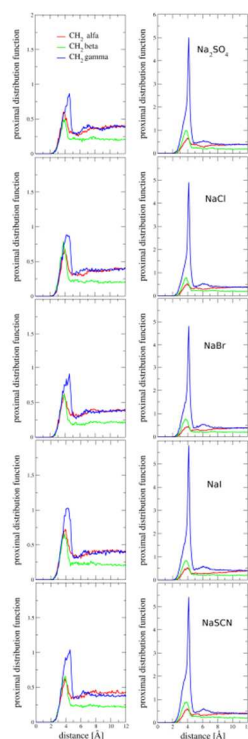


Figure S14: Proximal distribution functions of sodium cations around GGG tripeptide (left column - terminated GGG and right column - non-terminated GGG).

References

1. Hwan Kim, K.; Martin, Y.; Otis, E.; Mao, J. Inhibition of ^{125}I -labeled ristocetin binding to *Micrococcus luteus* cells by the peptides related to bacterial cell wall mucopeptide precursors: quantitative structure-activity relationships. *J. Med. Chem.* **1989**, 32, 84-93.
2. Eissmann, F.; Weber, E. Synthesis and structural characterization of amino acid and peptide derivatives featuring N-(p-bromobenzoyl) substituents as promising connection unit for bio-inspired hybrid compounds. *J. Mol. Struct.* **2011**, 994, 392-402.
3. Nandi, P.K.; Robinson, D.R. Effects of salts on the free energy of the peptide group. *J. Am. Chem. Soc.* **1972**, 94, 1299-1308.
4. Nandi, P.K.; Robinson, D.R. Effects of salts on the free energy of nonpolar groups in model peptides. *J. Am. Chem. Soc.* **1972**, 94, 1308-1315.
5. Computer Aided Resonance Assignment (CARA) software. <http://cara.nmr.ch>
6. Keller, R. Diss. ETH Nr. 15947.
7. Mix, G.; Schweitzer-Stenner, R.; Asher, S. A. Uncoupled adjacent amide vibrations in small peptides. *J. Am. Chem. Soc.* **2000**, 122, 9028-9029.
8. Lee, S. H.; Krimm, S. Ab initio-based vibrational analysis of alpha-poly(L-alanine). *Biopolymers* **1998**, 46, 283-317.
9. Barth, A.; Zscherp, C. What vibrations tell us about proteins. *Q. Rev. Biophys.* **2002**, 35, 369-430.
10. Kim, M. K.; Martell, A. E. Infrared spectra of aqueous solutions. IV. Glycine and glycine peptides. *J. Am. Chem. Soc.* **1963**, 85, 3080-3083.
11. von Hippel, P.H.; Peticolas, V.; Schack, L.; Karlson, L. Model studies on the effects of neutral salts on the conformational stability of biological macromolecules. I. Ion binding to polyacrylamide and polystyrene columns. *Biochemistry* **1973**, 12, 1256-1264.